Saturable absorption properties and femtosecond mode-locking application of titanium trisulfide

Wenjun Liu (iD), Mengli Liu, Ximei Liu (iD), Xiaoting Wang, Hao Teng, Ming Lei, Zhongming Wei (iD), and Zhiyi Wei

View Online   Export Citation   CrossMark

ARTICLES YOU MAY BE INTERESTED IN

Progress, challenges, and perspective on metasurfaces for ambient radio frequency energy harvesting
Applied Physics Letters **116**, 060501 (2020); https://doi.org/10.1063/1.5140966

Tunable valleytronics with symmetry-retaining high polarization degree in SnS_xSe_{1-x} model system
Applied Physics Letters **116**, 061105 (2020); https://doi.org/10.1063/1.5128717

Enhanced surface superconductivity in $Ba(Fe_{0.95}Co_{0.05})_2As_2$
Applied Physics Letters **116**, 062601 (2020); https://doi.org/10.1063/1.5133647

116, 061901

Saturable absorption properties and femtosecond mode-locking application of titanium trisulfide

Wenjun Liu,[1,2] (iD) Mengli Liu,[1] Ximei Liu,[1] (iD) Xiaoting Wang,[3] Hao Teng,[2] Ming Lei,[1,a)] Zhongming Wei,[3] (iD) and Zhiyi Wei[2,a)]

AFFILIATIONS

[1]State Key Laboratory of Information Photonics and Optical Communications, School of Science, Beijing University of Posts and Telecommunications, P.O. Box 91, Beijing 100876, China
[2]Beijing National Laboratory for Condensed Matter Physics, Institute of Physics, Chinese Academy of Sciences, Beijing 100190, China
[3]State Key Laboratory of Superlattices and Microstructures, Institute of Semiconductors, Chinese Academy of Sciences and Center of Materials Science and Optoelectronics Engineering, University of Chinese Academy of Sciences, Beijing 100083, China

[a)]Authors to whom correspondence should be addressed: mlei@bupt.edu.cn and zywei@iphy.ac.cn

ABSTRACT

Titanium trisulfide (TiS_3) is regarded as a candidate material for optoelectronic devices and nano-transistors due to its photoresponse. However, its nonlinear optical response in a mode-locked laser is yet to be investigated. Here, the performance of TiS_3 as a saturable absorber in a mode-locked laser is demonstrated. The generated mode-locked pulses achieve pulse duration as short as 147.72 fs at 1555 nm, which indicates that TiS_3 as a potential functional material has applications in nanomaterial-related photonics.

Published under license by AIP Publishing. https://doi.org/10.1063/1.5128725

It is generally considered that the discovery of graphene lays a foundation for the research of two-dimensional (2D) materials.[1,2] From then on, some kinds of 2D materials have begun to rise and have become research hotspots in the fields of photonics and optoelectronics.[3–5] There is still a long way to go for 2D materials as mature integrated circuit devices in terms of manufacturing technology, cost, reliability, and performance. However, as single independent devices, 2D materials have prominent performance in optical modulation and optical detection.[6–8] The miniaturization of 2D materials makes them more flexible for applications, and their optical and photoelectric properties such as high nonlinearity and ultrafast carrier dynamics improve the performance of optoelectronic devices.[9,10]

At present, some 2D materials, such as graphene,[11–13] transition metal dichalcogenides (TMDs),[14–17] topological insulators[18–21] and black phosphorus,[22–25] have achieved remarkable performance in the application of optical modulation devices. In particular, TMDs, as a large family that includes more than 40 different materials uniformly expressed as MX_2 (M: Mo, W, etc; X: S, Se, etc.), have been explored.[26] In TMDs, the adjacent individual layers bond together by weak van der Waals forces, which is propitious to the exfoliation of monolayer or few-layer forms.[27] Taking MoS_2 as an example, bulk MoS_2 exhibits an indirect bandgap of 1.29 eV, while eventually it shows a direct bandgap of 1.80 eV as the thickness decreases to monolayer.[28] Some

research highlights the photoelectric properties of MoS_2, including the photoluminescence in MoS_2 layers,[29] the on/off ratio exceeding 1×10^8, a mobility of $\sim$200 cm^2 V^{-1} s^{-1} in the field-effect transistor,[30] a third-order nonlinear optical susceptibility of $\sim$10^{-15} esu higher than that of graphene,[31] and a broadband nonlinear response covering 1–2 μm.[32]

TiS_3, as a semiconducting chalcogenide material similar to TMD material MoS_2, also possesses a thickness-related bandgap structure. The bulk TiS_3 exhibits an indirect bandgap of 0.94 eV, and the monolayer TiS_3 has an indirect bandgap of 1.02 eV.[33] However, TiS_3 shows strong anisotropy due to different crystal symmetries.[34] The optical responses in different polarization directions up to 4:1 originating from in-plane optical selection induced by strong anisotropy have generated widespread interest. What is more, TiS_3 exhibits on/off ratios of up to $\sim$7000 and a mobility of 43 cm^2 V^{-1} s^{-1} and can be a candidate material for optoelectronic devices and nanotransistors.[35] In the previous work, the application of TiS_3 in Q-switched lasers has been discussed.[36] However, using TiS_3, the mode-locked lasers with femtosecond pulses have not been demonstrated. Such femtosecond pulses have advantages in material precision machining, femtosecond time spectroscopy, and nanoimaging. This motivation leads us to explore the performance of TiS_3 in the mode-locked lasers with femtosecond pulses.

Here, the generation of femtosecond pulses from the mode-locked fiber lasers based on the TiS_3 saturable absorber (SA) is reported. TiS_3 SA is fabricated by chemical vapor transport (CVT) technology and shows optical nonlinearity at 1555 nm. After the employment of the TiS_3 SA in the fiber laser, the stable mode-locked operation at 1555 nm is demonstrated. The pulse duration of the mode-locked laser is as short as 147.72 fs. The good performance of lasers enables us to emphasize the applicability of TiS_3 as a feasible SA candidate in mode-locked lasers and explore more photonic applications.

TiS_3 here was prepared by CVT technology, in which the metastable phase single crystal is able to be obtained by temperature gradient transmission. After material preparation, the subsequent transfer process was performed. Detailed transfer processes have been illustrated in a previous report.[37] The atomic force microscopy (AFM) image in Fig. 1(a) shows the surface topography of the TiS_3 nanosheet. By comparing the difference in thickness between the reference plane and the top surface of TiS_3 in Fig. 1(a), the thickness of the TiS_3 film was ~182 nm. Because the TiS_3 material produced by the CVT technology in our experiments was needle-shaped, it was difficult to reconcile the demands of large size and few layers. Although it falls outside the scope of our ability at present due to the crystal size produced by our growth process, it is attractive to investigate the thickness-related saturable absorption of TiS_3 in the future.

Although the thickness of TiS_3 was 182 nm, it is different from the general bulk TiS_3. On the one hand, TiS_3 was obtained by further using the mechanical exfoliation method after the CVT method, which indicates that the dimensionality of TiS_3 is further reduced in the

preparation process. On the other hand, TiS_3 with a thickness of 182 nm showed the same properties in the Raman spectrum as the layered TiS_3 as shown in Fig. 1(b), which is consistent with a previous report.[38] The two peaks representing the interior vibration of TiS_3 were located at 300 (II: $A_g^{internal}$) and 371 cm^{-1} (III: $A_g^{internal}$). The peak at 558 cm^{-1} showed the vibration characteristics of S–S pairs. The peak displayed at 522 cm^{-1} was mainly Si derived from the substrate.[39] Ignoring the influence of the base element, it is known from the vibration mode peaks belonging to TiS_3 in the Raman spectrum that TiS_3 was prepared.

Figure 1(c) shows the absorption characteristics of TiS_3 in the near-infrared range. It is worth noting that TiS_3 exhibited 32% transmittance at 1550 nm. A Tauc plot from the data in Fig. 1(c) is shown in Fig. 1(d), which indicates that the bandgap of TiS_3 was estimated to be 0.58 eV. The range of wavelengths incident on TiS_3 was from 950 to 1800 nm. The experimental value of 0.58 eV was different from the theoretical value of 1.05 eV. According to previous studies, the reduction of the bandgap may be caused by the defect state.[40] This defect states in TiS_3 are likely to be introduced through the production process. Yu et al. demonstrated that the MoS_2 bandgap can be reduced from 1.08 to 0.08 eV by introducing the defects in a suitable range.[41] This reduction in bandgap is believed by some researchers to be a plausible cause for subband absorption. Therefore, it can be concluded that the decrease in the bandgap of TiS_3 is caused by some defects, which results in the absorption of TiS_3 at 1550 nm. The carrier dynamic relaxation process of TiS_3 is shown in Fig. 1(e). In the pump-probe measurement, the 500 nm pump beam has a pulse energy of 2.2 μJ and a diameter of 250 μm. The 800 nm pulse with a diameter of 120 μm was used to generate a white light continuum probe beam. After theoretical fitting, the relaxation time was as short as 1.34 ps, which indicates the potential applications of TiS_3 in ultrafast photonics. The optical nonlinearity of the TiS_3 SA, which is represented by power-dependent transmission characteristics, was measured by a balanced twin-detector method. The detailed process has been introduced in a previous report.[42] The results and fitting curve are shown in Fig. 1(f). The unsaturated loss as low as ~6% indicated the small insertion loss of the TiS_3 SA. The modulation depth was up to 39.39%, which aroused our curiosity about its performance in lasers. The light source of measurement was a home-made mode-locked laser operating at 1550 nm with a pulse duration of 700 fs.

As shown in Fig. 2(a), the Er-doped fiber laser (EDFL) that was constructed from single-mode fiber-integrated components was established. Optical devices including an isolator (ISO) that keeps light unidirectional propagating, a 20:80 output coupler (OC) for spectral and temporal monitoring, a segment of 0.6 m EDF (Liekki 110–4/125) used to enhance light intensity, and a polarization controller (PC) that is capable of fine tuning the polarization state and net cavity birefringence were all integrated into a typical ring cavity. The assembled
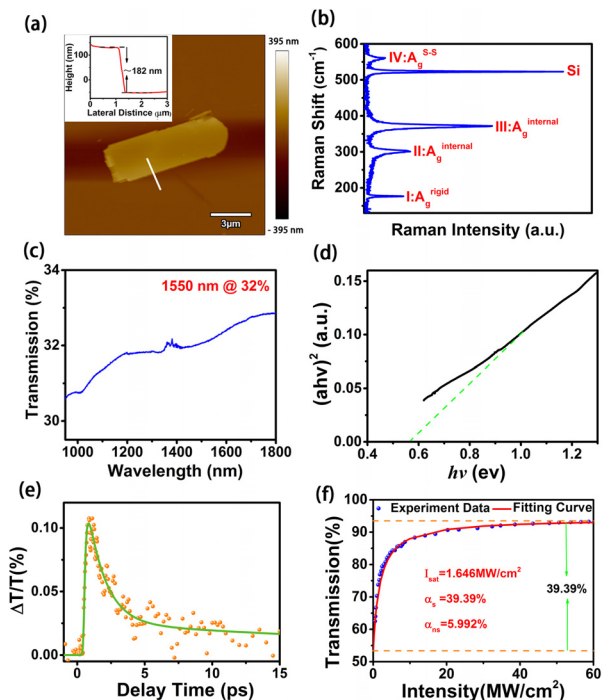

FIG. 1. (a) AFM micrograph, (b) Raman spectrum, (c) absorption spectrum, (d) Tauc plot, (e) transmittivity transients, and (f) absorption characteristics of TiS_3.

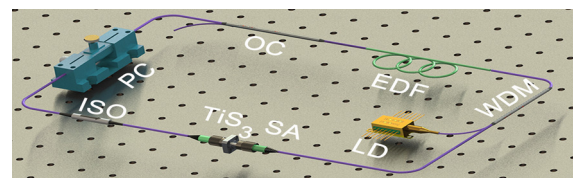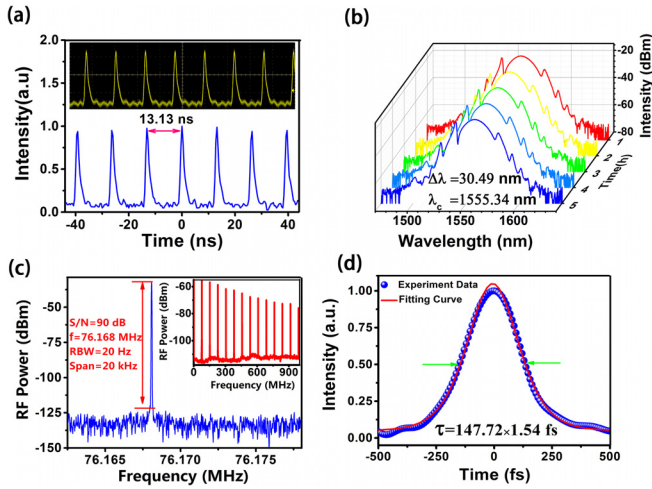**FIG. 2.** EDFL based on the TiS_3 SA.

FIG. 3. Performance of EDFL based on the TiS$_3$ SA: (a) pulse train, (b) spectrum, (c) RF spectrum, and (d) pulse duration.

FIG. 4. (a) Trend of output power of the EDFL change with different pump powers. (b) Output power monitoring within 15 h.

system was pumped by a commercial 980 nm laser diode (LD) through a 980/1550 nm wavelength division multiplexor (WDM). Prepared TiS$_3$ SA was placed after ISO for the verification experiment of optical nonlinearity.

Stable mode-locked pulse trains were observed using a real-time monitoring oscilloscope by properly adjusting PC at a pump power of 210 mW. During the sustained pump growth, the mode-locked state remained stable. The waveforms observed on an oscilloscope are collected in Fig. 3 when the pump power increased to a limited power of 630 mW. The mode-locked pulse train showed a uniform time interval of 13.13 ns in Fig. 3(a), and the repetition frequency corresponding to this time interval was in agreement with the experimental data of 76.168 MHz. It was observed from the spectrum that the center wavelength of the system located at 1555.34 nm with a wide 3-dB bandwidth of 30.49 nm in Fig. 3(b). The radio frequency (RF) spectrum with a resolution bandwidth of 20 Hz and a span of 20 kHz, which is considered to be able to reflect the stability of the system, is shown in Fig. 3(c). The signal-to-noise ratio (SNR) of fundamental frequency was up to 90 dB, which indicates that the fluctuation of amplitude is low. Moreover, from the wide monitoring span up to 1 GHz, no
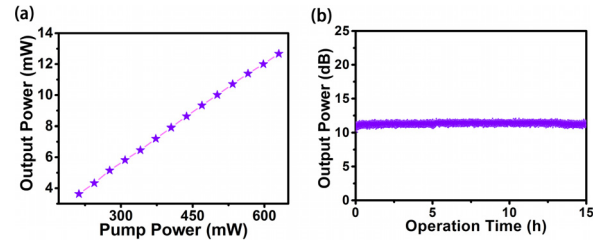
noticeable sign was observed from cavity harmonics in the inset of Fig. 3(c), which implies the stability of the system. The actual pulse shape was determined using an autocorrelator. By the sech^2 fitting for pulse in Fig. 3(d), the pulse duration of mode-locked pulses was revealed to be as short as 147.72 fs. According to the information of the spectrum and pulse duration, the time bandwidth product of the mode-locked system was calculated to be 0.5582. It was confirmed that the saturable absorption characteristics came from the TiS$_3$ SA. When the TiS$_3$ SA was replaced by the single mode fiber with the same length or fiber ferrules without TiS$_3$, the mode-locked pulses cannot be obtained, which indicates that the nonlinearity of the TiS$_3$ SA was the main reason for realizing the mode-locking of the fiber laser. Figure 4(a) shows the trend of output power of EDFL changing with pump power. The mode-locking threshold of EDFL was 210 mW. The maximum output power of EDFL was 12.67 mW. As the pump power increased, the rate of increase in output power was almost constant. There was no power stagnation or sudden change due to partial damage, which indicates that this SA works normally at higher power. When the incident power remained at the maximum of 630 mW, the output performance of the laser was monitored for a long time as shown in Fig. 4(b). It was observed that the output power of EDFL within 15 h was almost in a straight line, and there was no obvious power jump. The standard deviation of the power obtained by taking the dots at one second intervals within 15 h was 0.193 mW, and the corresponding dispersion was 1.7%, which indicates that the laser is stable. The efficiency (pump power/output power) of this EDFL is 2%.

In order to further evaluate the performance of the TiS$_3$ SA intuitively, some types of sulfides are listed for comparison in Table I. From the data summarized above, the TiS$_3$ SA performed well in

TABLE I. Performance comparison of EDFLs based on some sulfides.

Materials	MD(%)	$\triangle\lambda/\lambda$(nm)	SNR(dB)	τ (fs)	P(mW)	Efficiency	References
TiS$_2$	8.3	4.75/1563.3	60	812	…	…	26
Graphene	11	48/1545	65	88	1.5	1.4%	43
MoS$_2$	35.4	2.6/1568.9	62	1280	5.1	3.4%	44
	2.5	12.38/1568	61	637	…	…	45
WS$_2$	0.95	2.3/1557	>50	1320	…	…	46
	5.1	14.5/1565.5	~70	21 100	1.8	2.1%	47
ReS$_2$	0.12	1.85/1559	<60	1600	0.4	0.95%	48
SnS$_2$	4.6	6.09/1562.01	>45	623	1.2	0.59%	49
TiS$_3$	39.39	30.49/1555.34	90	147.72	12.67	2%	This work

EDFL due to the optical nonlinearity. In our experiments, the modulation depth of the prepared TiS_3 SA was up to 39.39%, and the pulse duration realized in the experiment was as short as 147.72 fs, which is consistent with the trend reported in previous reports.[49] According to Ref. 50, the pulse duration decreased with the increase in the modulation depth in theory. Regarding the SNR of 90 dB, our laser possessed better stability than mentioned lasers in Table I. Moreover, the TiS_3-based laser remained stable at relatively high power, showing the potential to be designed for high-power applications.

In summary, the TiS_3 SA with a modulation depth of 39.39% has been fabricated by the CVT technology. After the application of prepared TiS_3 SA with strong saturable absorption in the fiber laser, the ultrashort pulse as short as 147.72 fs has been obtained. Moreover, compared with similar sulfides, the system has performed well in terms of stability and power durability. The results highlight the development potential of TiS_3 as a promising functional material in various photon applications, especially the generation of ultrashort pulses.

REFERENCES

[1]K. Novoselov, A. Geim, S. Morozov, D. Jiang, Y. Zhang, S. Dubonos, I. Grigorieva, and A. Firsov, Science **306**, 666 (2004).

[2]K. Novoselov, A. Geim, S. Morozov, D. Jiang, M. Katsnelson, I. Grigorieva, S. Dubonos, and A. Firsov, Nature **438**, 197 (2005).

[3]K. Novoselov, A. Mishchenko, A. Carvalho, and A. C. Neto, Science **353**, aac9439 (2016).

[4]W. Choi, N. Choudhary, G. Han, J. Park, D. Akinwande, and Y. Lee, Mater. Today **20**, 116 (2017).

[5]Z. Sun, A. Martinez, and F. Wang, Nat. Photonics **10**, 227 (2016).

[6]G. Hu, T. Owen, X. Jin, A. Ali, Y. Hu, R. Howe, K. Shehzad, Z. Yang, X. Zhu, R. Woodward, T. Wu, H. Jussila, J. Wu, P. Peng, P. Tan, Z. Sun, E. Kelleher, M. Zhang, Y. Xu, and T. Hasan, Nat. Commun. **8**, 278 (2017).

[7]P. Yan, A. Liu, Y. Chen, J. Wang, S. Ruan, H. Chen, and J. Ding, Sci. Rep. **5**, 12587 (2015).

[8]W. Liu, M. Liu, J. Yin, H. Chen, W. Lu, S. Fang, H. Teng, M. Lei, P. Yan, and Z. Wei, Nanoscale **10**, 7971 (2018).

[9]F. Liu, H. Shimotani, H. Shang, T. Kanagasekaran, V. Zólyomi, N. Drummond, V. Fal'ko, and K. Tanigaki, ACS Nano **8**, 752 (2014).

[10]M. Zhang, G. Hu, G. Hu, R. Howe, L. Chen, Z. Zheng, and T. Hasan, Sci. Rep. **5**, 17482 (2015).

[11]Q. Bao, H. Zhang, Y. Wang, Z. Ni, Y. Yan, Z. Shen, K. Loh, and D. Tang, Adv. Funct. Mater. **19**, 3077 (2009).

[12]H. Zhang, D. Tang, L. Zhao, Q. Bao, and K. Loh, Opt. Express **17**, 17630 (2009).

[13]K. Peng, C. Wu, Y. Lin, H. Wang, C. Cheng, Y. Chi, and G. Lin, Nanophotonics **7**, 207 (2018).

[14]K. Wu, C. Guo, H. Wang, X. Zhang, J. Wang, and J. Chen, Opt. Express **25**, 17639 (2017).

[15]Y. Xie, B. Zhang, S. Wang, D. Wang, A. Wang, Z. Wang, H. Yu, H. Zhang, Y. Chen, M. Zhao, B. Huang, L. Mei, and J. Wang, Adv. Mater. **29**, 1605972 (2017).

[16]H. Li, H. Xia, C. Lan, C. Li, X. Zhang, J. Li, and Y. Liu, IEEE Photonic. Tech. Lett. **27**, 69 (2015).

[17]G. Wang, S. Zhang, X. Zhang, L. Zhang, Y. Cheng, D. Fox, H. Zhang, J. Coleman, W. Blau, and J. Wang, Photonics Res. **3**, A51 (2015).

[18]P. Yan, R. Lin, S. Ruan, A. Liu, and H. Chen, Opt. Express **23**, 154 (2015).

[19]H. Yu, H. Zhang, Y. Wang, C. Zhao, B. Wang, S. Wen, H. Zhang, and J. Wang, Laser Photonics Rev. **7**, L77–L83 (2013).

[20]H. Zhang, C. Liu, X. Qi, X. Dai, Z. Fang, and S. Zhang, Nat. Phys. **5**, 438 (2009).

[21]J. Sotor, G. Sobon, W. Macherzynski, P. Paletko, K. Grodecki, and K. Abramski, Opt. Mater. Express **4**(1), 1 (2014).

[22]D. Na, K. Park, K. Park, and Y. Song, Nanotechnology **28**, 475207 (2017).

[23]R. Zhang, Y. Zhang, H. Yu, H. Zhang, R. Yang, B. Yang, Z. Liu, and J. Wang, Adv. Opt. Mater. **3**, 1787 (2015).

[24]A. Rodin, A. Carvalho, and A. Neto, Phys. Rev. Lett. **112**, 176801 (2014).

[25]C. Han, M. Yao, X. Bai, L. Miao, F. Zhu, D. Guan, and Y. Liu, Phys. Rev. B **90**, 085101 (2014).

[26]X. Zhu, S. Chen, M. Zhang, L. Chen, Q. Wu, J. Zhao, Q. Jiang, Z. Zheng, and H. Zhang, Photonics Res. **6**, C44 (2018).

[27]A. Geim and I. Grigorieva, Nature **499**, 419 (2013).

[28]R. Woodward and E. Kelleher, Appl. Sci. **5**, 1440 (2015).

[29]A. Splendiani, L. Sun, Y. Zhang, T. Li, J. Kim, C. Chim, G. Galli, and F. Wang, Nano Lett. **10**, 1271 (2010).

[30]B. Radisavljevic, A. Radenovic, J. Brivio, V. Giacometti, and A. Kis, Nat. Nanotechnol. **6**, 147 (2011).

[31]K. Wang, J. Wang, J. Fan, A. Lotya, A. O'Neill, D. Fox, Y. Feng, X. Zhang, B. Jiang, Q. Zhao, H. Zhang, J. Coleman, L. Zhang, and W. Blau, ACS Nano **7**, 9260 (2013).

[32]Z. Luo, Y. Huang, M. Zhong, Y. Li, J. Wu, B. Xu, H. Xu, Z. Cai, J. Peng, and J. Weng, J. Lightwave Technol. **32**, 4679 (2014).

[33]J. Wu, D. Wang, H. Liu, W. Lau, and L. Liu, RSC Adv. **5**, 21455 (2015).

[34]J. Island, M. Buscema, M. Barawi, J. Clamagirand, J. Ares, C. Sánchez, I. Ferrer, G. Steele, H. Zant, and A. Gomez, Adv. Opt. Mater. **2**, 641 (2014).

[35]A. Lipatov, P. Wilson, M. Shekhirev, J. Teeter, R. Netusil, and A. Sinitskii, Nanoscale **7**, 12291 (2015).

[36]H. Hou, T. You, Q. Zhou, M. Liu, Y. Ouyang, X. Liu, and W. Liu, Optik **205**, 164234 (2020).

[37]W. Liu, M. Liu, X. Wang, T. Shen, G. Chang, M. Lei, H. Deng, Z. Wei, and Z. Wei, ACS Appl. Nano Mater. **2**, 2697 (2019).

[38]A. Pawbake, J. Island, E. Flores, J. Ares, C. Sanchez, I. Ferrer, S. Jadkar, H. van der Zant, A. Castellanos-Gomez, and D. Late, ACS Appl. Mater. Interfaces **7**, 24185 (2015).

[39]R. Kobliska and S. Solin, Phys. Rev. B **8**, 3799 (1973).

[40]D. Mao, B. Du, D. Yang, S. Zhang, Y. Wang, W. Zhang, X. She, H. Cheng, H. Zeng, and J. Zhao, Small **12**, 1489 (2016).

[41]S. Wang, H. Yu, H. Zhang, A. Wang, M. Zhao, Y. Chen, L. Mei, and J. Wang, Adv. Mater. **26**, 3538 (2014).

[42]M. Liu, Y. OuYang, H. Hou, M. Lei, W. Liu, and Z. Wei, Chin. Phys. B **27**, 084211 (2018).

[43]J. Sotor, I. Pasternak, A. Krajewska, W. Strupinski, and G. Sobon, Opt. Express **23**, 27503 (2015).

[44]H. Xia, H. Li, C. Lan, C. Li, X. Zhang, S. Zhang, and Y. Liu, Opt. Express **22**, 17341 (2014).

[45]R. Khazaeizhad, S. Kassani, H. Jeong, D. Yeom, and K. Oh, Opt. Express **22**, 23732 (2014).

[46]D. Mao, Y. Wang, C. Ma, L. Han, B. Jiang, X. Gan, S. Hua, W. Zhang, T. Mei, and J. Zhao, Sci. Rep. **5**, 7965 (2015).

[47]D. Mao, S. Zhang, Y. Wang, X. Gan, W. Zhang, T. Mei, Y. Wang, Y. Wang, H. Zeng, and J. Zhao, Opt. Express **23**, 27509 (2015).

[48]D. Mao, X. Cui, X. Gan, M. Li, W. Zhang, H. Lu, and J. Zhao, IEEE J. Sel. Top. Quantum Electron. **24**, 1100406 (2018).

[49]K. Niu, R. Sun, Q. Chen, B. Man, and H. Zhang, Photonics Res. **6**, 72 (2018).

[50]J. Jeon, J. Lee, and J. H. Lee, J. Opt. Soc. Am. B **32**, 31 (2015).